International Journal of Geosynthetics and Ground Engineering (2020) 6:25
https://doi.org/10.1007/s40891-020-00211-4

ORIGINAL PAPER

Experimental Investigation on Dynamic Characterization of Equi-Proportionate Silt–Sand Range Pond Ash at High Strain

M. V. Ravi Kishore Reddy[1] · Supriya Mohanty[2] · S. Rehana[1]

Received: 1 February 2020 / Accepted: 20 May 2020 / Published online: 2 June 2020

Abstract
In the present study, it was attempted to investigate the cyclic resistance of equi-proportionate silt–sand range pond ash (with 50% fines) at relatively high shear strains using the strain-controlled cyclic triaxial test. The cyclic triaxial tests have been performed considering the effect of relative compaction (97–99%), cyclic shear strain (0.6–1.35%), frequency of loading (0.3–1 Hz) and effective confining pressure (50–100 kPa) on cyclic resistance of pond ash. Dynamic characteristics such as dynamic shear modulus and damping ratio of equi-proportionate silt–sand range pond ash was evaluated for all the parameters considered at high shear strain. The maximum value of the dynamic shear modulus and damping ratio of pond ash observed in this study was 6534.8 kPa and 23.64%, respectively. The dynamic shear modulus and damping ratio of pond ash was decreased from 6534.8 to 5023.87 kPa and 23.64 to 14.17% with the increase in shear strain amplitude from 0.6 to 1.35%. Besides, few relationships were established between the amount of energy dissipated until liquefaction and parameters influencing liquefaction using an energy concept.

Keywords Pond ash · Cyclic resistance · High shear strain · Strain-controlled cyclic triaxial test · Dynamic shear modulus · Damping ratio

Introduction

The studies on characterization of coal ash reported by several researchers facilitated its utilization in various areas such as embankments, retaining walls, stowing material in mines, landfills, stabilization of expansive soil, as a superficial layer over soil, etc. [1–9]. The utilization of ash generated from the thermal power stations (TPS) in India was around 63.28% (155 TPS) and 67.13% (167 TPS) for the years 2016–2017 and 2017–2018, respectively [10, 11]. Out of this utilized ash, the percentage of ash used for ash dyke raising, reclamation of low-lying areas and mine backfilling constitute only 20.5% and 23.75% for the years 2016–2017 and 2017–2018, respectively. This attributes to the conservation of soil by utilizing coal ash. However, utilization of coal ash may lead to the instability of fill material under dynamic loading conditions. This demands a detailed study on dynamic characterization and liquefaction potential evaluation of coal ash in seismic prone regions. The liquefaction potential of coal ash can be evaluated by performing laboratory studies (cyclic triaxial tests, shake table tests, resonant column tests, centrifuge tests, etc.) and numerical analysis using finite element methods.

It has been observed from the laboratory studies (resonant column and cyclic triaxial tests) that due to irregular grain structure, particle morphology and mineralogy, calcareous sand possesses high shear modulus, low damping ratio than that of siliceous sand [12]. It was noticed from the stress-controlled cyclic triaxial tests performed on various mixtures of sand-fines that with the addition of fines the dynamic shear modulus of the mixture reduces significantly at low

This the 13th PAPER of Special Issue (SI) to be published as the ORIGINAL PAPER S.I.: Materials and Processes for Ground Engineering Infrastructure.

✉ Supriya Mohanty
supriya.civ@iitbhu.ac.in

M. V. Ravi Kishore Reddy
meegada.reddy@research.iiit.ac.in

S. Rehana
rehana.s@iiit.ac.in

[1] Earthquake Engineering Research Centre, International Institute of Information Technology Hyderabad, Telangana 500032, India

[2] Department of Civil Engineering, Indian Institute of Technology (BHU) Varanasi, Varanasi 221005, India

strain loading [13]. In addition, from cyclic direct simple shear tests, it was found that threshold strain to generate pore pressure in silty sands increases with the increase in fine content [14]. The liquefaction susceptibility of medium dense sand through experimental (strain controlled cyclic triaxial tests) and numerical (Proshake) studies were investigated recently by Hazirbaba and Omarow [15]. The reduction in excess pore pressure development and liquefaction susceptibility in soil was noticed from the centrifuge tests conducted by reducing the degree of saturation of the soil sample [16]. The investigation on pond ash subjected to moderate-to-strong earthquakes using small shake table tests in laboratory exhibited non-liquefiable state (pore pressure ratio, $r_{umax} < 1$) due to the presence of more fines (nearly 35%) [17]. Few researchers conducted resonant column tests on fly ash to determine its dynamic properties and influencing factors like aging effect, confining pressure and strain amplitude [18, 19]. The provision of geosynthetic reinforcement in fly ash increases its liquefaction resistance as observed from the cyclic triaxial tests conducted by Boominathan and Hari [20]. The liquefaction resistance of pond ash from different seismic zones was investigated by conducting strain-controlled cyclic triaxial tests by Mohanty and Patra [21]. Jakka et al. [22] performed extensive studies on cyclic resistance of pond ash considering different sample location from ash ponds. Few researchers [23–28] performed studies on dynamic characterization and liquefaction evaluation of sand/coal ash using cyclic triaxial tests. Many researchers have performed several numerical studies on seismic performance of layered soil/pond ash deposits with shallow foundation [29–31], seismic performance of embankments with pond ash [32, 33] and seismic ground response analysis of pond ash [34].

Few researchers have developed several methods for the assessment of liquefaction potential [35–37]. It has been noticed that the initiation of pore pressure built-up and collapse of particle structure causes decay in cyclic strength and stiffness of the sample above a certain threshold value of stress or strain amplitude during cyclic loading [38]. The accurate measurement of pore pressure during cyclic loading is a challenge for samples of an equal percentage of silt and sand range particles. During the cyclic test, the pore pressure can be measured from either top/bottom or middle of the sample, which may disturb the structure of the sample. To equalize pore pressure effectively in fine ash specimens during cyclic test frequency value of 0.01 Hz was adopted in the past studies [21]. However, pore pressure cannot be generated uniformly over a deposit as loading frequency of earthquake waves would be much higher than that adopted in a laboratory test. Therefore, for seismic conditions, it may not be reliable to evaluate the liquefaction potential of pond ash having an equal percentage of silt and sand range particles using pore pressure parameter.

The conventional stress-based [35] and strain-based [36] methods of liquefaction analysis need either equivalent uniform cyclic stress or the number of cycles of loading to simulate the actual earthquake conditions for analysis. Instead of those methods, the energy approach would be an ideal choice for evaluating the cyclic resistance of pond ash mainly during non-uniform loading, as this method is independent of loading waveforms [39]. Many researchers used energy concepts to determine the cyclic resistance of soil deposits [40, 41]. Studies conducted by Nemat and Shookh [42] on sand led to an idea of energy concept and they found that the energy required to generate excess pore pressure can be related to dissipated energy obtained from the hysteresis loop. During a loading cycle, the area covered under hysteresis loop is expressed as energy per unit volume in the energy concept method.

Most of the researchers studied the liquefaction phenomenon of pond ash consisting mostly of sand range particles without or with little silt or clay range particles. It is of keen interest to study the cyclic behaviour of pond ash with a predominant percentage of silt or clay range particles subjected to high strains. Hence, in this study, cyclic strength performance of silt–sand range (equi-proportionate) pond ash was investigated under high shear strains. Besides, the energy concept was adopted to establish some relationships between energy dissipated in the pond ash sample until liquefaction and parameters influencing liquefaction potential of pond ash. The relationships between energy dissipated and the response of pond ash against cyclic loading has been developed using Eq. (1).

The energy dissipated (ΔW) in the pond ash specimen until it gets liquefied is given by [39]:

$$\Delta W = \sum_{i=1}^{n-1} \frac{1}{2}\left(\sigma_i + \sigma_{i+1}\right)\left(\varepsilon_{i+1} - \varepsilon_i\right), \tag{1}$$

where σ: deviator stress, ε: axial strain and n: number of points recorded until liquefaction.

Fundamental Geotechnical Properties of Pond Ash

The pond ash used in this study was collected from an intermediate point between disposal point and outflow point of Talcher thermal power station (TTPS) ash pond, Odisha, India that lies in the seismic zone–III (moderate seismic intensity) [43]. The ash samples have been collected at a depth of 0.5 m below the ground surface. Here, extensive laboratory cyclic triaxial tests were performed for determining the dynamic characteristic and cyclic resistance of equi-proportionate silt–sand range pond ash.

Initially, few fundamental geotechnical properties such as specific gravity, grain size, maximum dry unit weight and optimum moisture content of pond ash were determined for further detailed study. The specific gravity of present pond ash (1.85) was observed to be within the range of Indian pond ash [44]. The present pond ash contains both silt (51%) and sand (49%) range particles (Fig. 1). The gradation of the sample varies with time and location of the collection in an ash pond [22]. The maximum dry unit weight and optimum moisture content of the collected pond ash sample was found to be 10.76 kN/m^3 and 33.5%, respectively. Though pond ash contains almost equi-proportionate silt–sand range particles, the presence of a predominant range of fine ash particles by a little margin forced researchers to adopt relative compaction in this study. The ratio of required dry unit weight in the field to the maximum dry unit weight of sample obtained from the laboratory is termed as relative compaction. The minimum requirement of compaction of subgrade material of the embankment should not be less than 97% relative compaction and moisture content of the given material should be within + 1 to − 2% of optimum moisture content [45]. Hence, in this study, it was decided to adopt different relative compaction i.e. from 97 to 99% to replicate the field conditions of the pond ash utilization under foundations, as the subgrade material in embankments, etc. and to determine the response of the pond ash under cyclic loading condition.

Methodology of Cyclic Triaxial Tests

The pond ash collected in the present study was of equi-proportionate sand–silt range particles, which was of keen interest to be investigated for its dynamic characteristics. Multiple sets of strain-controlled cyclic triaxial tests were conducted to examine the cyclic strength of collected pond ash at different strain levels tested under different effective confining pressures, frequencies and relative compaction. The flowchart of multiple sets of cyclic triaxial tests performed on collected pond ash sample is shown in Fig. 2. The strain-controlled cyclic triaxial test was selected as it can establish a fundamental assessment of pond ash response with strain level, which can influence the generation of pore pressure and provides an actual realistic prediction of on-site pore pressure generation.

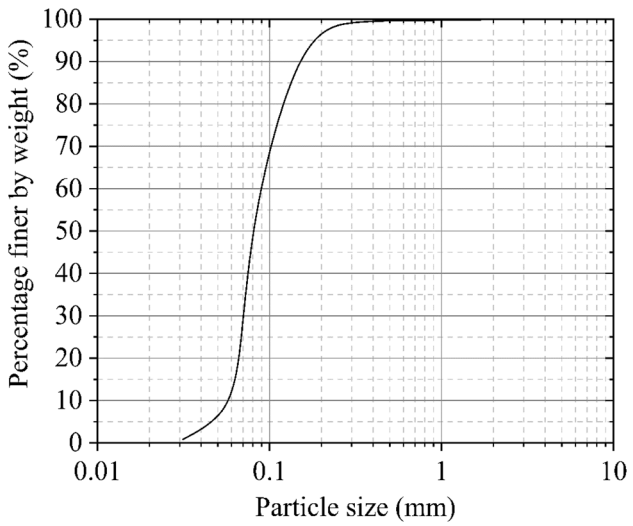

Fig. 1 Particle size distribution curve of pond ash

Test Procedure for Cyclic Triaxial Test

The consolidated undrained cyclic triaxial tests (strain-controlled) were performed on the collected pond ash samples. The preparation of pond ash specimen and adopted set of varying parameters have been discussed briefly in the following sections.

Preparation of Specimen

The specimen of size 50 mm (diameter) × 100 mm (height) was prepared using a conventional moist tamping method. The pond ash sample was compacted in layers into a mould. Each layer was compacted by hand tamping to achieve the desired relative compaction of the specimen. The detailed procedure of specimen preparation has been described in the following paragraphs.

The pond ash specimen was prepared in three to five layers of compaction. After the compaction of all the layers, a plunger was used on either end of the mould to level the specimen. Then, the compacted specimen was extracted from the mould with the utmost care using sample extruder. The specimen was then placed over the porous disc (rested on the triaxial cell pedestal) with filter paper at the bottom of the specimen. Similarly, a filter paper and a porous disc were placed over the specimen. The specimen was then sealed by a rubber membrane with O-rings at the top and bottom of the specimen. When the B (pore pressure parameter) value reaches beyond 0.95, then the saturation stage was stopped and consolidation under a desired effective confining pressure was started. After consolidation, the shearing of the specimen was done by applying desired cyclic strain amplitudes. The details of considered parameters for the current study were stated in the following paragraph.

The pond ash specimen was subjected to strain-controlled sinusoidal loading using digitally controlled cyclic triaxial test equipment. All the tests were performed according to the guidelines of ASTM D5311 [46] and ASTM D3999 [47]. The specimens prepared at different relative compaction (RC: 97%, 98% and 99%) were subjected to sinusoidal loading with cyclic shear strain amplitudes of 0.6%, 0.9%,

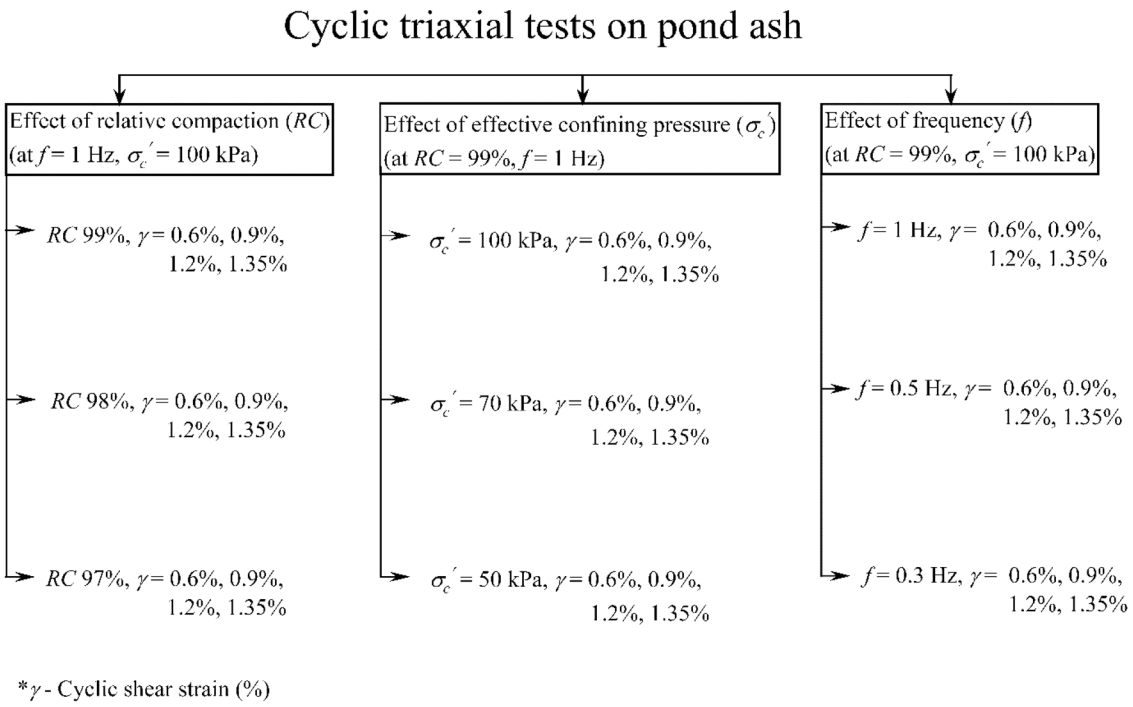

Fig. 2 Flowchart of sets of cyclic triaxial tests performed on pond ash

1.2% and 1.35%; frequency of loading of 0.3 Hz, 0.5 Hz and 1 Hz and effective confining pressures of 50 kPa, 70 kPa and 100 kPa. Multiple sets of tests were performed with different combinations as stated above and shown in Fig. 2. All the cyclic triaxial test results of pond ash specimens were recorded and extracted using the system intended for data collection. The dynamic shear modulus (G_{dyn}) and damping ratio (D) of pond ash samples were calculated using the following Eqs. (2–4) and Fig. 3.

$$E = \sigma_d/\varepsilon, \tag{2}$$

$$\gamma = (1+\nu)\varepsilon \text{ and } G_{dyn} = E/2(1+\nu), \tag{3}$$

$$D = A_L/\left(4\pi A_T\right), \tag{4}$$

where E: Young's modulus, σ_d: deviator stress, ε: axial strain, γ: shear strain, υ: Poisson's ratio, A_L: area enclosed by the hysteresis loop and A_T: area of the shaded triangle.

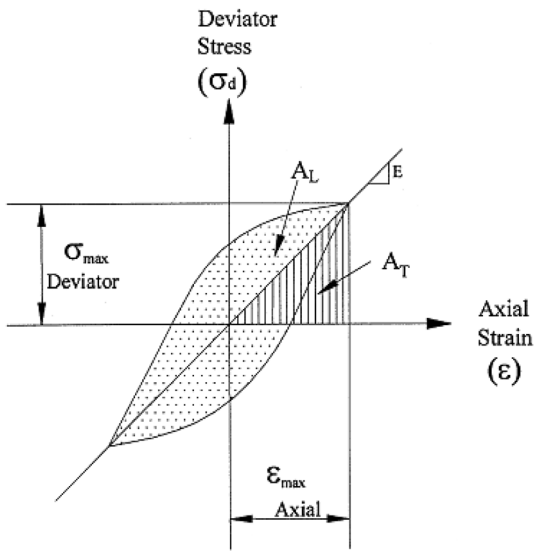

Fig. 3 Hysteretic stress–strain relationship for cyclic loading

Results and Discussion

Multiple sets of cyclic triaxial tests were performed to investigate the cyclic resistance of pond ash material. These multiple sets comprise different relative compaction of pond ash, set of loading frequency and range of effective confining pressure.

The progress of cyclic loading on pond ash specimen leads to lower its stiffness, which in turn causes a decrease in the area of hysteresis loop as shown in Fig. 4. With an increase in loading cycles, the pond ash specimen fails to sustain as a solid structure and complete loss of deviator stress was noticed. During initial cycles of loading, the pond

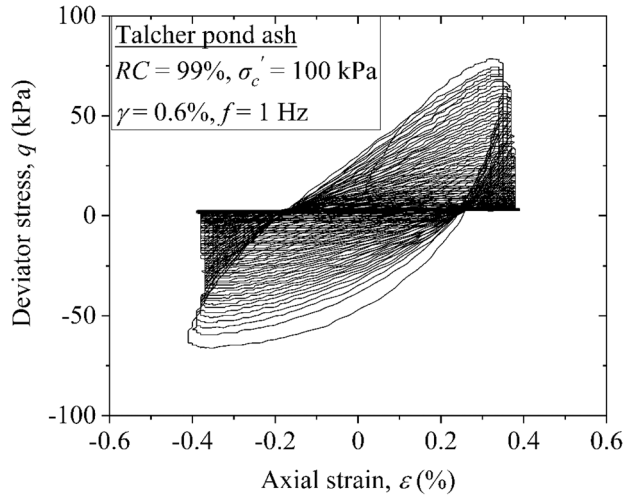

Fig. 4 Variation of deviator stress with axial strain of pond ash specimen prepared with RC = 99% tested at $\sigma_c' = 100$ kPa, $f = 1$ Hz and $\gamma = 0.6\%$

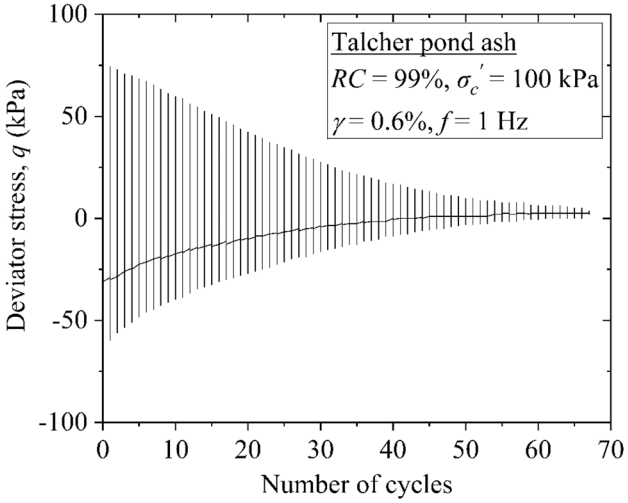

Fig. 6 Variation of deviator stress with number of cycles of pond ash specimen prepared with RC = 99% tested at $\sigma_c' = 100$ kPa, $f = 1$ Hz and $\gamma = 0.6\%$

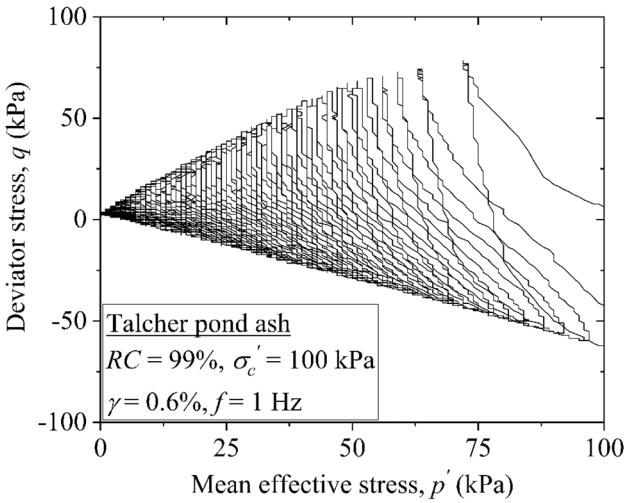

Fig. 5 Variation of deviator stress with mean effective stress of pond ash specimen prepared with RC = 99% tested at $\sigma_c' = 100$ kPa, $f = 1$ Hz and $\gamma = 0.6\%$

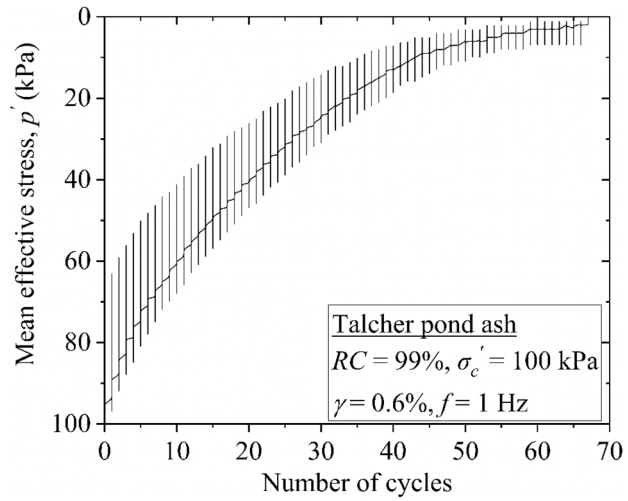

Fig. 7 Variation of effective stress with number of cycles of pond ash specimen prepared with RC = 99% tested at $\sigma_c' = 100$ kPa, $f = 1$ Hz and $\gamma = 0.6\%$

ash specimen shows a resistance against deformation. The increase in the loading cycle causes a gain in pore water pressure under the undrained conditions. The faster rate of development of pore pressure causes a reduction in inter-particle stresses and a state exists where no longer particles maintain contact with each other. In other words, the occurrence of complete loss of effective stress can be noticed when the pore pressure approaches its initial confining pressure as represented in Fig. 5. At this stage, the initiation of liquefaction of pond ash specimen was noticed. As there is gradual loss of effective stress over the number of loading cycles, the pond ash specimen can sustain no load at the end of the last cycle of loading where liquefaction was observed (Figs. 6, 7). The number of loading cycles caused initial liquefaction of pond ash specimen represents its potential to liquefy. In general, the best way to express the occurrence of liquefaction is when the pore pressure ratio approaches one as presented in Fig. 8.

Effect of Varying Parameters on Dynamic Characteristics of Pond Ash

The variation of dynamic shear modulus and damping ratio exhibited by the reconstituted pond ash specimens against

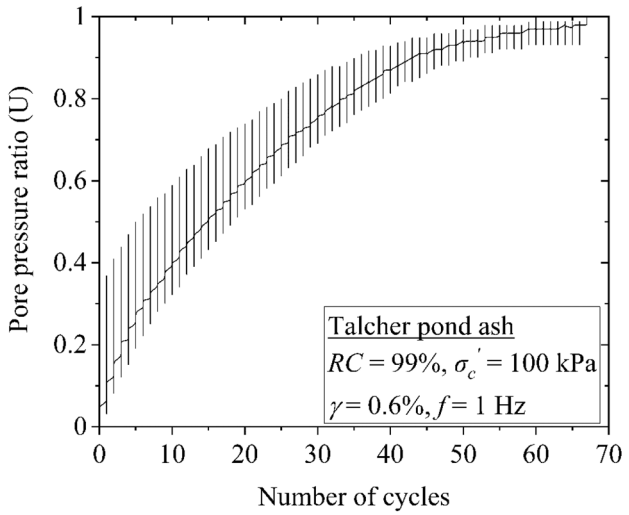

Fig. 8 Variation of pore pressure ratio with number of cycles of pond ash specimen prepared with RC = 99% tested at $\sigma_c' = 100$ kPa, $f = 1$ Hz and $\gamma = 0.6\%$

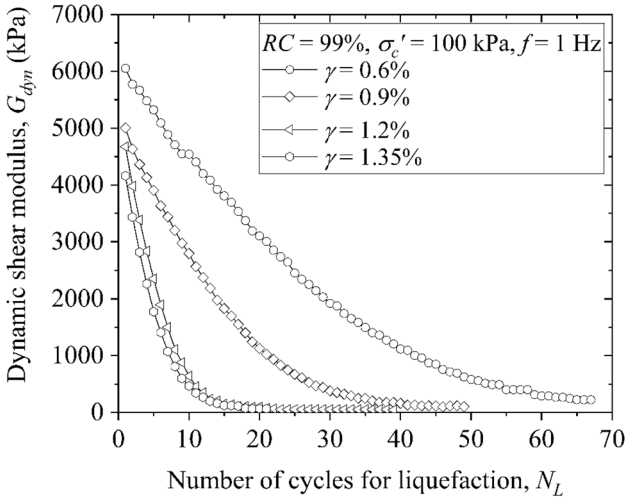

Fig. 9 Variation of dynamic shear modulus (G_{dyn}) with number of cycles of pond ash specimen prepared with RC = 99% tested at $\sigma_c' = 100$ kPa, $f = 1$ Hz for different amplitudes of cyclic shear strains (0.6%, 0.9%, 1.2% and 1.35%)

all varying parameters adopted in this study is investigated in this section. The selection of relative compaction closest to maximum dry unit weight was considered to know the effect of relative compaction on dynamic characteristics of pond ash (97%, 98% and 99% RC). In the past study, high frequency (1 Hz) was adopted for coarse ash specimens (containing predominant sand range particles); and low frequency (0.1 Hz) was adopted for fine ash specimens (containing predominant silt range particles) to provide enough time for pore pressure generation equally over the specimen [22]. However, in this study, moderate-to-high frequency (0.3–1 Hz) was deliberately selected to investigate the behaviour of pond ash under moderate-to-high frequency range. The effective confining pressure of 50–100 kPa was considered to represent the shallow depth (4.6–9.3 m) of pond ash deposit in the field. All the tests were performed under the cyclic shear strain amplitudes of 0.6%, 0.9%, 1.2% and 1.35%.

The decay in dynamic shear modulus (G_{dyn}) was progressive with the number of loading cycles. In addition, the decay in G_{dyn} was rapid with the enhancement of cyclic shear strain (Fig. 9). The presence of 50% fines and high compacted state of pond ash specimen cause close packing of particles, which offers more resistance to shear strain; this results in possession of the high shear modulus as observed in this study. It is well known that the susceptibility of liquefaction is more at shallow depth than that at greater depth. The same was observed in this study that the pond ash specimen subjected to high effective confining pressure possesses less tendency to liquefaction (Table 1). Also, it was concluded from the test results that pond ash specimen takes a greater number of cycles to liquefy at low frequency. The number of cycles for liquefaction of pond ash specimen of the most densified state in this study was 87 at a low frequency of loading i.e. 0.3 Hz (Table 1). Previous studies [39] state that there was a little effect or no effect of frequency on cyclic resistance of the specimen, but results obtained in this study exhibit a clear effect of frequency on cyclic resistance of pond ash. However, no significant trend of dynamic shear modulus with varying frequency was noticed against $\gamma \leq 0.9\%$ in this study (Table 2). The maximum value of damping ratio (i.e. 23.64%) was obtained for the highly compacted specimen (RC 99%) confined at high pressure (100 kPa) subjected to high frequency (1 Hz) at 0.6% cyclic shear strain. A decrement trend of damping ratio was noticed with the amplification in shear strain from 0.6 to 1.35%. The presence of 50% fines in the present pond ash specimen makes the specimen to exhibit less G_{dyn} (i.e. 33% less) than that of past studies of Mohanty and Patra [21]. In this study, the variation of dynamic shear modulus with relative compaction, loading frequency, effective confining pressure and cyclic shear strain was in good agreement with the past studies on pond ash, fly ash and sandy soils [18, 21, 48–50]. Also, the damping ratio obtained in this study was less than half of that obtained in the past study [21]. It is due to the presence of predominant sand range particles in the pond ash of past study where specimen offers appreciable resistance to loading. The presence of predominant silt range particles (51%) make the specimen to offer less resistance against the applied high strains despite better interlocking of silt and sand range particles of compacted pond ash specimen in the present study. High shear strains cause silt range particles to move sideways and separated upon loading which results in the lower shear modulus of

Table 1 Number of cycles (N_L) required for liquefaction

Relative compaction, RC (%)	Effective confining pressure, σ_c' (kPa)	Frequency, f (Hz)	Number of cycles for liquefaction (N_L)			
			Cyclic shear strain, γ (%)			
			0.60%	0.90%	1.20%	1.35%
99% ($e-0.737$)	100	1	67	51	40	22
98% ($e-0.754$)	100	1	57	42	30	19
97% ($e-0.772$)	100	1	56	33	26	16
99% ($e-0.737$)	100	1	67	51	40	22
99% ($e-0.737$)	70	1	61	45	30	20
99% ($e-0.737$)	50	1	58	40	21	19
99% ($e-0.737$)	100	1	67	51	40	22
99% ($e-0.737$)	100	0.5	74	70	52	41
99% ($e-0.737$)	100	0.3	87	86	70	66

specimen [51]. It can be inferred from the conclusions that the dynamic characteristics depend on the inter-grain contact pressure distribution, which was evident from the studies of Thevanayagam et al. [52] on several kinds of sandy and silty soils. However, the observed values of damping ratio were in contrast with that of the past studies on pond ash tested for similar adopted parameters [21] and contrary to the studies on different kinds of sandy soils [38, 53]. The damping ratio of fly ash with a predominant range of silt particles (~80%) was found to be increased with an increase in shear strain [48]; this observation is in contrast to the present study. It was noticed from the past studies that the damping ratio gets diminished beyond 0.5% cyclic shear strain [50], which is in good agreement with the current study. A similar trend was noticed from the past studies on sandy soils, cohesive soils by many researchers [27, 54–57]. The variation of G_{dyn} and its gradual loss with cyclic strain for different relative compaction, frequency and effective confining pressure can be illustrated in Figs. 10, 11 and 12. Also, the uncertainty of damping ratio noticed from the test results against various parameters can be seen in Figs. 13, 14 and 15. In addition, the number of cycles for liquefaction with shear strain is presented in Table 1.

Degradation of Dynamic Shear Modulus of Pond Ash

The degradation of dynamic shear modulus with loading cyclic was termed as degradation index (δ) which represents the ratio of dynamic shear modulus in each cycle to the observed dynamic shear modulus in the first cycle of loading. It is necessary to examine the degradation index of the pond ash material thoroughly before its utilization in the field for various purposes. The degradation index represents the decay in shear strength of a material subjected to cyclic loads. From the results of the present study, it was clear that the rate of decrease in dynamic shear modulus was faster between 3 and 45 cycles of loading and thereafter it continues with a slower rate. It was also noticed that 50% degradation of the dynamic shear modulus occurred within 4–28 cycles of loading. The trend of results in this section represents the swift response of the pond ash to applied cyclic load. The pond ash sample investigated in this study loses its shear strength and approaches the initiation of liquefaction at a smaller number of loading cycles. The effect of parameters such as relative compaction, effective confining pressure and loading frequency on degradation index of pond ash has been represented in Figs. 16, 17 and 18, respectively.

Variation of Dynamic Shear Modulus over Number of Loading Cycles

In this section, the number of loading cycles, i.e. 5 and 10 cycles were chosen to represent a point of significance like an earthquake event (viz., M_w: 7.0) [34, 35] for the demonstration of the variation of dynamic shear modulus over number of loading cycles. It was noticed that the higher the density of the specimen, the slower is the drop in dynamic shear modulus of the pond ash specimen. The decrease in the strength of the ash specimen was observed with the progress in cycles of loading. For a high-density pond ash specimen (RC 99%) subjected to a cyclic shear strain, loading frequency and effective confining pressure of 0.6%, 1 Hz and 100 kPa, respectively, the percentage reduction in dynamic shear modulus was 12.07% at the end of 5 cycles of loading. However, at the end of ten cycles of loading, the reduction in dynamic shear modulus was just above twice of that observed for five cycles. The percentage reduction in dynamic shear modulus of pond ash at the end of five cycles of loading was in the range of 12–64% with an increment of cyclic shear strain amplitude from 0.6 to 1.35% of the considered set of relative compaction, loading frequency and confining pressure i.e. 97–99%, 0.3–0.5 Hz and 50–100 kPa, respectively. Similarly, at the end of ten cycles, it lay in the

Table 2 Variation of dynamic shear modulus (G_{dyn}) over number of cycles

Parameters maintained constant	Parameters varied	Dynamic shear modulus, G_{dyn} (kPa)											
		$\gamma-0.60\%$			$\gamma-0.90\%$			$\gamma-1.20\%$			$\gamma-1.35\%$		
		1 cycle	5 cycles	10 cycles	1 cycle	5 cycles	10 cycles	1 cycle	5 cycles	10 cycles	1 cycle	5 cycles	10 cycles
$\sigma_c^{'}-100$ kPa, $f-1$ Hz	RC − 99%	6053.47	5322.37	4542.37	5002.82	3906.1	2794.37	4674.06	2354.81	642.06	4161.67	1774.38	467.33
	RC − 98%	5820.52	4863.55	3900	4756.35	2903.88	1372.88	4479.61	1599.08	293.82	4394.5	1803.16	417.3
	RC − 97%	5745.90	4891.92	3953.74	4258.77	2751.37	1349.42	3700	1784.71	475.78	3298.85	1077.2	207.49
RC − 99%, $f-1$ Hz	$\sigma_c^{'}-100$ kPa	6053.47	5322.37	4542.37	5002.82	3906.1	2794.37	4674.06	2354.81	642.06	4161.67	1774.38	467.33
	$\sigma_c^{'}-70$ kPa	5158.25	4368.63	3596.34	4683.18	3453.85	2209.88	4200	2350.60	891.80	3530.35	1429.1	369.88
	$\sigma_c^{'}-50$ kPa	4168.92	3329.16	2680.50	4080.32	2978.34	1921.03	3927.90	1894.80	587.65	3356.28	1552.97	381.50
RC − 99%, $\sigma_c^{'}-100$ kPa	$f-1$ Hz	6053.47	5322.37	4542.37	5002.82	3906.1	2794.37	4674.06	2354.81	642.06	4161.67	1774.38	467.33
	$f-0.5$ Hz	6436.93	5627.84	5023.19	6335.88	4777.47	3500.47	5313.43	3516.57	1872.89	4656.14	2806.52	1275.69
	$f-0.3$ Hz	6534.80	5611.69	4837.15	6032.73	4358.84	2819.32	5587.64	3890	2394.70	5023.87	3189.23	1687.90

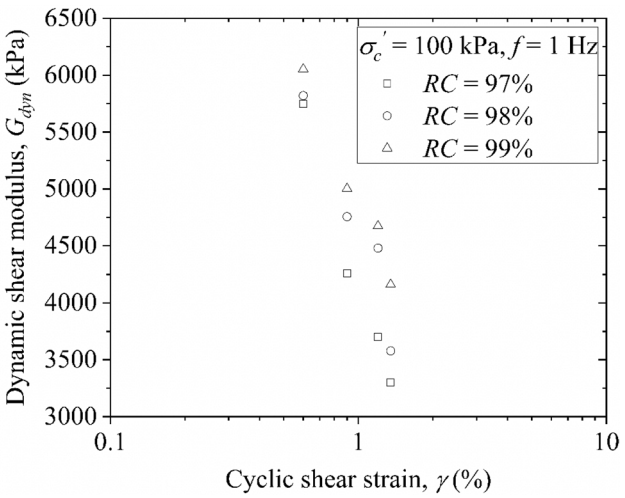

Fig. 10 Variation of dynamic shear modulus (G_{dyn}) with cyclic shear strain (γ) of pond ash specimen tested at $\sigma_c^{'}=100$ kPa and $f=1$ Hz representing effect of relative compaction (97%, 98% and 99%)

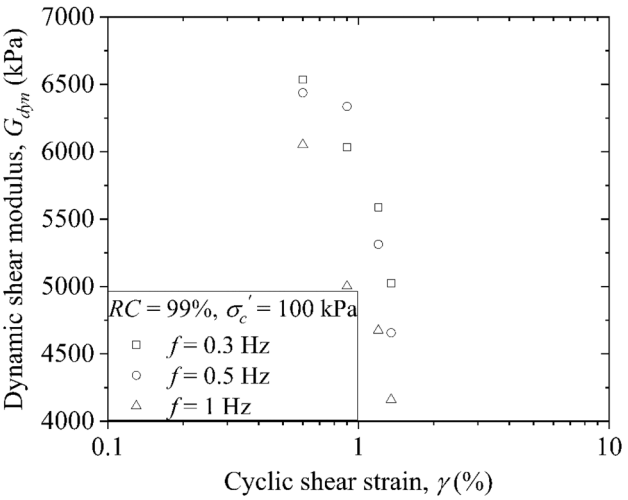

Fig. 11 Variation of dynamic shear modulus (G_{dyn}) with cyclic shear strain (γ) of pond ash specimen prepared with RC = 99% tested at $\sigma_c^{'}=100$ kPa representing effect of loading frequency (0.3 Hz, 0.5 Hz and 1 Hz)

range of 22–94%. This shows that the pond ash specimen of equi-proportionate silt–sand range when subjected to high strain loading ($\gamma>0.9\%$), the strength of the specimen appears to be diminished (more than 50%) in early stages of loading. Also, at the high cyclic shear strain ($\gamma=1.35\%$), the dynamic shear modulus got reduced to a maximum value of 94% at the end of ten cycles of loading. These observations thus give researchers much scope to work on the utilization of pond ash by improving its strength to sustain high strain loading. It becomes a prime concern to improve the status of construction activities involving coal ash as a better replacement of soil. The variation of dynamic shear modulus over

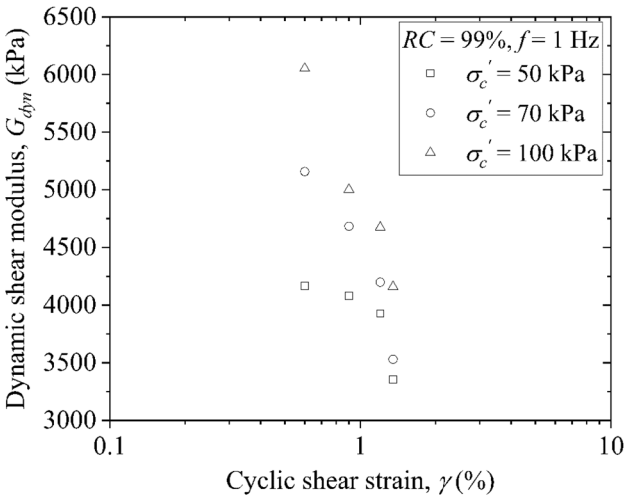

Fig. 12 Variation of dynamic shear modulus (G_{dyn}) with cyclic shear strain (γ) of pond ash specimen prepared with RC = 99% tested at f = 1 Hz representing effect of effective confining pressure (50 kPa, 70 kPa and 100 kPa)

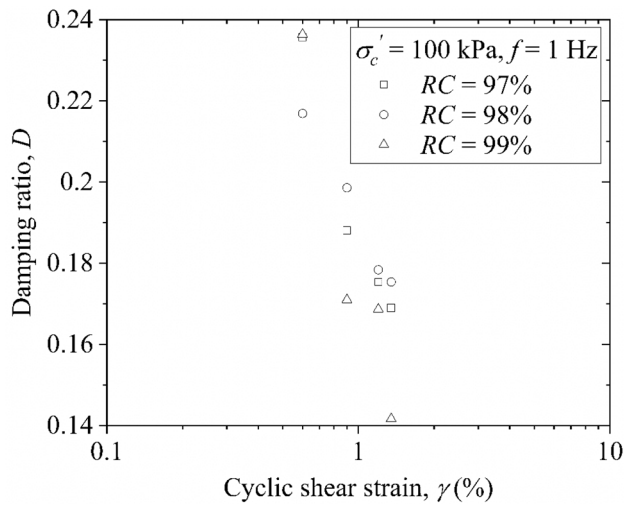

Fig. 13 Variation of damping ratio (D) with cyclic shear strain (γ) of pond ash specimen tested at σ_c' = 100 kPa and f = 1 Hz representing effect of relative compaction (97%, 98% and 99%)

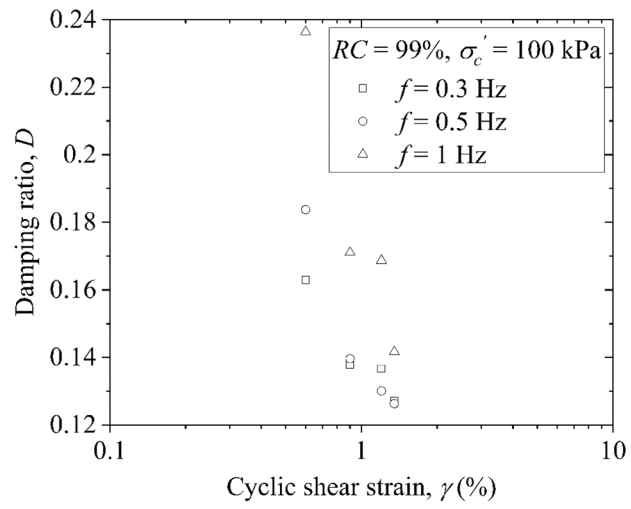

Fig. 14 Variation of damping ratio (D) with cyclic shear strain (γ) of pond ash specimen prepared with RC = 99% tested at σ_c' = 100 kPa representing effect of loading frequency (0.3 Hz, 0.5 Hz and 1 Hz)

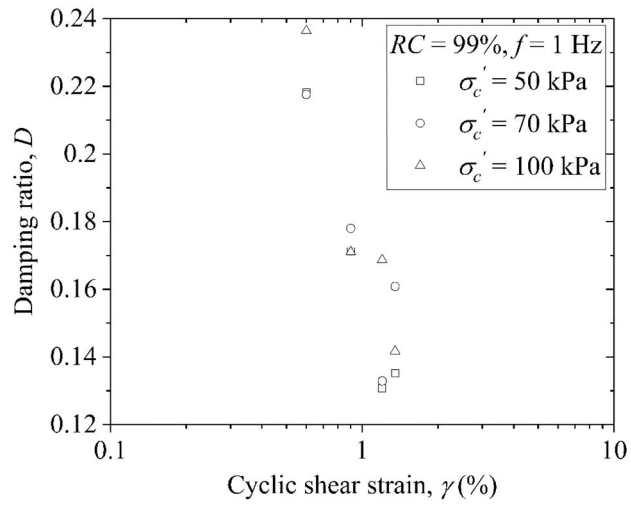

Fig. 15 Variation of damping ratio (D) with cyclic shear strain (γ) of pond ash specimen prepared with RC = 99% tested at f = 1 Hz representing effect of effective confining pressure (50 kPa, 70 kPa and 100 kPa)

considered number of cycles (1, 5, 10) for the interpretation of the strength of the pond ash has been presented in Table 2.

Relationships for Liquefaction Potential Evaluation of Pond Ash by Energy Method

Here, the energy method was adopted to establish a relation between energy dissipated in pond ash specimen until liquefaction and parameters influencing liquefaction. Irrespective of the type of tests performed (viz., stress controlled or strain controlled), the cyclic strength of pond ash can be evaluated with this method by evaluating the energy dissipated during cyclic loading until liquefaction.

The area inside a hysteresis loop (i.e. generated during a loading cycle) gives the energy associated with pore pressure generation under undrained condition. The area of hysteresis loop is a combination of both load and deformation, which is an advantage of this method and is observed unlike conventional stress-based or strain-based methods. The progress in cycles of loading until liquefaction results in a decrease in the area of hysteresis loop tending it becomes flattered at the end. This indicates the amount of dissipated

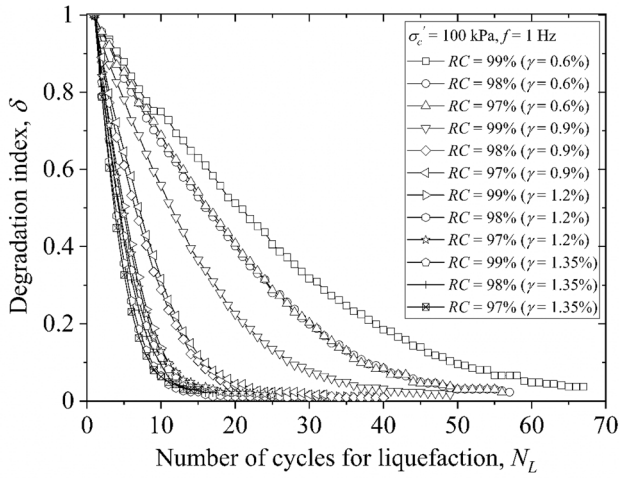

Fig. 16 Effect of relative compaction on degradation index (δ) of pond ash specimen

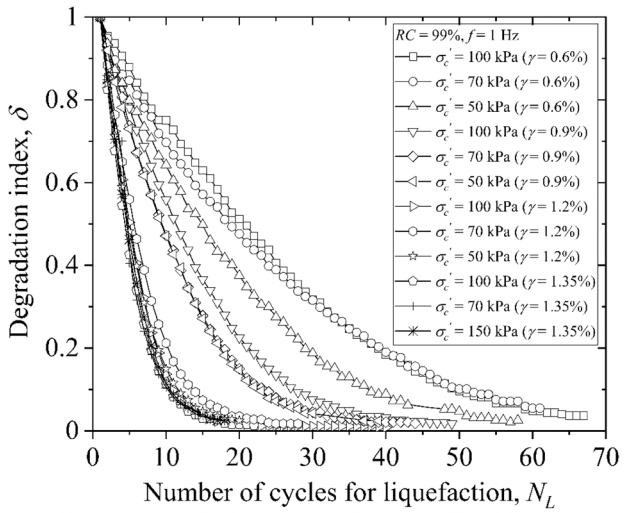

Fig. 17 Effect of effective confining pressure on degradation index (δ) of pond ash specimen

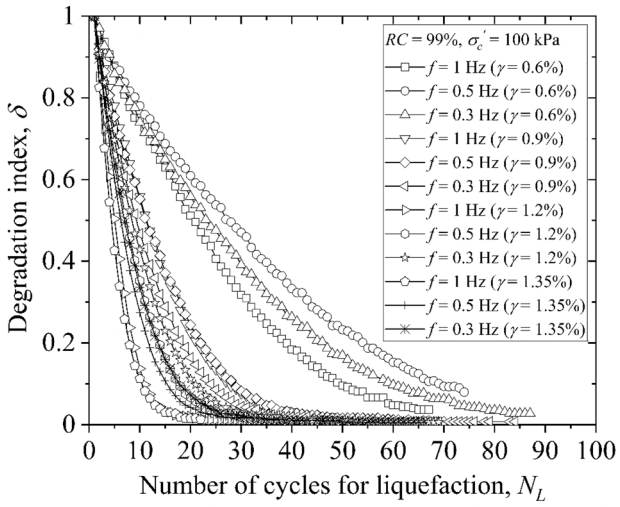

Fig. 18 Effect of loading frequency on degradation index (δ) of pond ash specimen

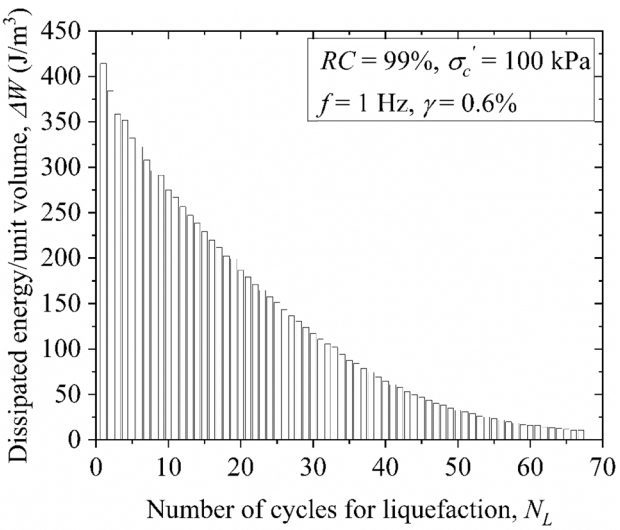

Fig. 19 Typical variation of dissipated energy/unit volume per each cycle until liquefaction of pond ash specimen prepared with RC = 99% tested at f = 1 Hz, γ = 0.6% and σ_c' = 100 kPa

energy was decreased with the progress in cycles of loading due to the increase in pore pressure generation (Fig. 19). This was due to the decrease in resistance of the specimen to deformation. The specimen withholds its strength from inter-particle resistance, which gets diminished with the rise in pore pressure and consequently decreases the effective stress, thus a state of liquefaction occurs. A typical representation of cumulative energy dissipated until the specimen gets liquefied has been presented in Fig. 20. It looks like the variation of the pore pressure ratio (Fig. 8) which inferred that flat end can be observed in both the plots representing the stage of cyclic failure. From this observation, it can be stated that an attempt of using this method was promising in this study. The amount of energy required to cause liquefaction and factors influencing it has been discussed in the following section.

The heavily compacted pond ash specimens dissipated high amount of energy until liquefaction with other parameters being constant. More energy was required to cause cyclic failure of the specimen when there was an increase in effective confining pressure with other parameters being constant. In addition, an increase in frequency requires more energy to cause complete loss of cyclic strength of the pond ash specimen. At 0.3 Hz frequency adopted in this study, the influence of cyclic shear strain (at 0.6% and 0.9%) on variation of energy dissipated to initiate liquefaction does

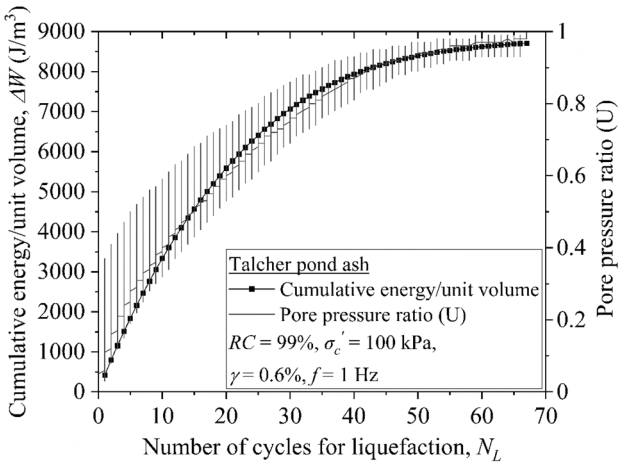

Fig. 20 Typical variation of cumulative dissipated energy/unit volume per each cycle until liquefaction of pond ash specimen prepared with RC = 99% tested at $f = 1$ Hz, $\gamma = 0.6\%$ and $\sigma_c' = 100$ kPa

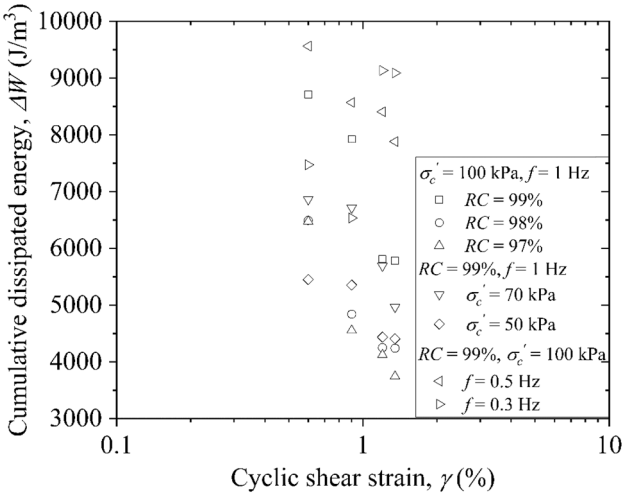

Fig. 21 Variation of cumulative dissipated energy with cyclic shear strain (γ) of pond ash specimen representing effect of relative compaction (99%, 98% and 97%), effective confining pressure (50 kPa, 70 kPa and 100 kPa), loading frequency (1 Hz, 0.5 Hz and 0.3 Hz)

not follow any trend with other results. The cyclic shear strain had its influence on energy dissipation over all the factors considered in this study (Fig. 21). The variation of energy dissipated over considered influencing factors has been presented in Table 3.

Also, it was observed that the dissipation of energy over the first few cycles of loading was rapid, and it continued with a decreasing trend afterwards. A regression analysis has been carried out for the results obtained and out of various analyses, i.e. linear, polynomial, logarithmic relationships, the relationships that provide the best fitting to the results have been presented here. The dependent variable was dissipated energy for triggering liquefaction with independent variables such as relative compaction (or void ratio), effective confining pressure, cyclic shear strain amplitude and loading frequency.

$$\log \Delta W = -5.436 + 0.093\mathrm{RC} + 0.0025\sigma_c' - 0.23\gamma;\quad R^2 = 0.85\left(\text{Considering } 'RC'\right), \tag{5}$$

$$\log \Delta W = 7.72 - 5.30e + 0.0024\sigma_c' - 0.23\gamma;\quad R^2 = 0.84\left(\text{Considering } 'e'\right), \tag{6}$$

$$\log \Delta W = -5.824 + 0.098\mathrm{RC} + 0.0026\sigma_c' - 0.155\gamma - 0.13f;\quad R^2 = 0.79\left(\text{Considering } 'RC'\right), \tag{7}$$

$$\log \Delta W = 7.95 - 5.55e + 0.0026\sigma_c' - 0.155\gamma - 0.13f;\quad R^2 \approx 0.79\left(\text{Considering } 'e'\right), \tag{8}$$

Equations (5) and (6) have been developed for the variables like dissipated energy (ΔW), relative compaction (RC) (or void ratio (e)), effective confining pressure (σ_c') and cyclic shear strain (γ), whereas Eqs. (7) and (8) involves loading frequency (f) along with previously stated variables. It can be noticed that, the variation in the coefficient of determination (R^2) was obvious by the inclusion of loading frequency, which holds the statement of the effect of frequency on energy dissipation of pond ash. The variation of observed results through experimental tests with predicted results using Eq. (7) has been presented in Fig. 22. It can be noticed from Fig. 22 that the percentage variation of observed and predicted results is $\pm 4\%$.

Conclusions

Multiple sets of cyclic triaxial tests were performed to investigate the dynamic characteristics of the equi-proportionate silt–sand range pond ash. The influence of relative compaction, effective confining pressure, cyclic shear strain and loading frequency on dynamic characteristics of pond ash have been explored in this study. The following inferences were drawn from the experimental test results:

- Reduction in the value of the dynamic shear modulus of pond ash was noticed with the increment of cyclic shear strain amplitude (0.6–1.35%) for all the varying parameters considered (relative compaction: 97–99%, confining pressure: 50–100 kPa and loading frequency: 0.3–1 Hz). The damping ratio of pond ash was observed to be decreased with varying high shear strains.
- The pond ash of the current study contains an equal proportion of silt and sand range particles (50% fine

Table 3 Summary of dissipated energy (J/m^3) required for triggering liquefaction

Relative compaction, RC (%)	Effective confining pressure, σ_c' (kPa)	Frequency, f (Hz)	Unit energy (J/m^3)			
			Cyclic shear strain, γ (%)			
			0.60%	0.90%	1.20%	1.35%
99% ($e-0.737$)	100	1	8710.5	7927.1	5808.2	5781.7
98% ($e-0.754$)	100	1	6491.9	4840.6	4248.9	4240.6
97% ($e-0.772$)	100	1	6475.2	4553	4121.8	3743.7
99% ($e-0.737$)	100	1	8710.5	7927.1	5808.2	5781.7
99% ($e-0.737$)	70	1	6862.2	6713.9	5689.3	4965.5
99% ($e-0.737$)	50	1	5449.4	5353	4436.6	4406.1
99% ($e-0.737$)	100	1	8710.5	7927.1	5808.2	5781.7
99% ($e-0.737$)	100	0.5	9564.4	8570.8	8408.3	7883.5
99% ($e-0.737$)	100	0.3	7472.9	6535.3	9134.7	9090.1

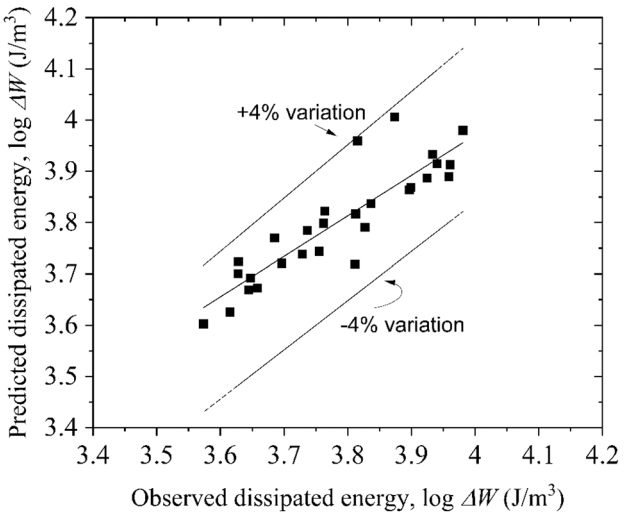

Fig. 22 Variation of predicted values of dissipated energy of pond ash with observed experimental results

particles), which results in less strength and tends to degrade at an early stage of loading cycles. The results of the study reveal that 50% decay of dynamic shear modulus occurs within 5–28 cycles of loading. In addition, the presence of non-plastic fines readily causes liquefaction.

- A significant influence of high cyclic shear strain amplitudes on dynamic characteristics of pond ash was observed, which provides a platform to evaluate the liquefaction potential for any form of loading that represents conditions of earthquake loading on the field.
- Relationships were established to quantify the amount of energy dissipated in a pond ash when subjected to cyclic loads. The cyclic strength of a pond ash deposit can be defined using such established relationships. A comparison can be made between energy dissipated to initiate liquefaction and the amount of energy generated by an earthquake excitation to assess the chance of occurrence of liquefaction.
- The present study is confined to a range of relative compaction, effective confining pressure, loading frequency and amplitudes of cyclic shear strain. Hence, it has much scope to investigate further for better inferences on the cyclic strength of pond ash.

Acknowledgements Authors are grateful to Department of Science and Technology, Government of India for providing financial assistance.

Funding This article was funded by Science and Engineering Research Board (ECR/2015/000580).

References

1. Mohapatra R, Kanungo SB (1997) Physico-chemical characteristics of fly ash samples from thermal power plants of Orissa. Indian J Eng Mater Sci 4:271–281. https://nopr.niscair.res.in/handle/123456789/29763
2. Kaniraj SR, Gayathri V (2004) Permeability and consolidation characteristics of compacted fly ash. J Energy Eng 130(1):18–43. https://doi.org/10.1061/(ASCE)0733-9402(2004)130:1(18)
3. Pandian NS (2004) Fly ash characterization with reference to geotechnical applications. J Indian Inst Sci 84:189–216
4. Das SK, Yudhbir (2005) Geotechnical characterization of some Indian fly ashes. J Mater Civ Eng 17(5):544–552. https://doi.org/10.1061/(ASCE)0899-1561(2005)17:5(544)
5. Kim B, Prezzi M, Salgado R (2005) Geotechnical properties of fly and bottom ash mixtures for use in highway embankments. J Geotech Geoenviron Eng 131(7):914–924. https://doi.org/10.1061/(ASCE)1090-0241(2005)131:7(914)
6. Bera AK, Ghosh A, Ghosh A (2007) Compaction characteristics of pond ash. J Mater Civ Eng 19(4):349–357. https://doi.org/10.1061/(ASCE)0899-1561(2007)19:4(349)

7. Jakka RS, Ramana GV, Dutta M (2010) Shear behavior of loose and compacted pond ash. Geotech Geol Eng 28:763–778. https://doi.org/10.1007/s10706-010-9337-1
8. Mishra DP, Das SK (2010) Study of physico-chemical and mineralogical properties of Talcher coal fly ash for stowing in underground coal mines. Mater Charact 61:1252–1259. https://doi.org/10.1016/j.matchar.2010.08.008
9. Mohanty S, Patra NR (2015) Geotechnical characterization of Panki and Panipat pond ash in India. Int J Geo-Eng 6(13):1–18. https://doi.org/10.1186/s40703-015-0013-4
10. Central Electricity Authority (2017) Report on fly ash generation at coal/lignite based thermal power stations and its utilization in the country for the year 2016–17. https://www.cea.nic.in/reports/others/thermal/tcd/flyash_201617.pdf. Accessed 18 Aug 2018
11. Central Electricity Authority (2018) Report on fly ash generation at coal/lignite based thermal power stations and its utilization in the country for the year 2017–18. https://www.cea.nic.in/reports/others/thermal/tcd/flyash_201718.pdf. Accessed 21 Dec 2018
12. Jaffarian Y, Javdanian H, Haddan A (2018) Dynamic properties of calcareous and siliceous sands under isotropic and anisotropic stress conditions. Soils Found 58:172–184. https://doi.org/10.1016/j.sandf.2017.11.010
13. Shivaprakash BG, Dinesh SV (2017) Dynamic properties of sand–fines mixtures. Geotech Geol Eng 35:2327–2337. https://doi.org/10.1007/s10706-017-0247-3
14. Hazirbaba K, Rathje EM (2009) Pore pressure generation of silty sands due to induced cyclic shear strains. J Geotech Geoenviron Eng 135(12):1892–1905. https://doi.org/10.1061/(ASCE)GT.1943-5606.0000147
15. Hazirbaba K, Omarow M (2019) Strain-based assessment of liquefaction and seismic settlement of saturated sand. Cogent Eng 6:1573788. https://doi.org/10.1080/23311916.2019.1573788
16. Zeybek A, Madabhushi SPG (2017) Centrifuge testing to evaluate the liquefaction response of air-injected partially saturated soils beneath shallow foundations. Bull Earthq Eng 15:339–356. https://doi.org/10.1007/s10518-016-9968-6
17. Singh HP, Maheshwari BK, Saran S, Paul DK (2008) Evaluation of liquefaction potential of pond ash. In: Proc 14th World Conf on Earthq Eng Beijing, pp 1–8
18. Chattaraj R, Sengupta A (2017) Dynamic properties of fly ash. J Mater Civ Eng 29(1):04016190. https://doi.org/10.1061/(ASCE)MT.1943-5533.0001712
19. Yu PJ, Qin WQ (1991) Dynamic properties of saturated coal fly ash. In: Proc Second Int Conf on Recent Adv Geotech Earthq Eng Soil Dyn Missouri, pp 27–32
20. Boominathan A, Hari S (2002) Liquefaction strength of fly ash reinforced with randomly distributed fibers. Soil Dyn Earthq Eng 22:1027–1033. https://doi.org/10.1016/S0267-7261(02)00127-6
21. Mohanty S, Patra NR (2014) Cyclic behavior and liquefaction potential of Indian pond ash located in seismic zones III and IV. J Mater Civ Eng 26:06014012. https://doi.org/10.1061/(ASCE)MT.1943-5533.0000964
22. Jakka RS, Datta M, Ramana GV (2010) Liquefaction behaviour of loose and compacted pond ash. Soil Dyn Earthq Eng 30:580–590. https://doi.org/10.1016/j.soildyn.2010.01.015
23. Paul S, Dey AK (2007) Cyclic triaxial testing of fully and partially saturated soil at Silchar. In: Proc 4th Int Conf Earthq Geotech Eng Thessaloniki, pp 1–12
24. Sitharam TG, Govindaraju L (2007) Pore pressure generation in silty sands during cyclic loading. Geomech Geoeng Int J 2(4):295–306. https://doi.org/10.1080/17486020701670460
25. Zand B, Tu W, Amaya PJ, Wolfe WE, Butalia TS (2009) An experimental investigation on liquefaction potential and post-liquefaction shear strength of impounded fly ash. Fuel 88:1160–1166. https://doi.org/10.1016/j.fuel.2008.10.020
26. Dingrando JS, Kalinski ME, Salehian A, Zand BB (2013) Cyclic triaxial testing of water pluviated fly ash specimens. In: Proc World of Coal Ash Conf Lexington, KY, pp 1–13
27. Kumar SS, Krishna AK, Dey A (2018) Dynamic properties and liquefaction behaviour of cohesive soil in North East India under staged cyclic loading. J Rock Mech Geotech Eng 10:958–967. https://doi.org/10.1016/j.jrmge.2018.04.004
28. Kumar SS, Dey A, Krishna AK (2018) Response of saturated cohesionless soil subjected to irregular seismic excitations. Nat Hazards 3312:1–21. https://doi.org/10.1007/s11069-018-3312-1
29. Mohanty S, Reddy MVRK (2016) Seismic analysis of shallow foundation on layered soil deposits. In: ACESC 2016 Proc Int conf Adv Civil Eng Sust Const Chennai, pp 532–537
30. Reddy MVRK, Mohanty S, Ramancharla PK (2019) Comparative study of dynamic response analysis of shallow foundation on layered soils. In: Adimoolam B, Banerjee S (eds) Soil dynamics and earthquake geotechnical engineering. Lecture notes in civil engineering, Springer, Singapore, pp 91–99. https://doi.org/10.1007/978-981-13-0562-7_11
31. Reddy MVRK, Mohanty S, Rehana S (2020) Seismic performance of soil-ash and soil-ash-foundation system: a parametric study. Int J Geotech Earthq Eng 11(1):45–70. https://doi.org/10.4018/IJGEE.2020010103
32. Mohanty S, Patra NR (2016) Dynamic response analysis of Talcher pond ash embankment in India. Soil Dyn Earthq Eng 84:238–250. https://doi.org/10.1016/j.soildyn.2016.01.021
33. Mohanty S, Patra NR (2016) Liquefaction and earthquake response analysis of Panipat pond ash embankment in India. J Earthq Tsunami 10(2):1650009. https://doi.org/10.1142/S1793431116500093
34. Reddy MVRK, Mohanty S, Rehana S (2018) Comparative study of 1D, 2D and 3D ground response analysis of pond ash from Odisha under different earthquake motions. In: Proc Indian Geotech Conf Bengaluru, pp 1–8
35. Seed HB, Idriss LM (1971) Simplified procedure for evaluating soil liquefaction potential. ASCE J Soil Mech Found Div 97(9):1249–1274
36. Dobry R, Ladd RS, Yokel FY, Chung RM, Powell D (1982) Prediction of pore water pressure build-up and liquefaction of sands during earthquakes by the cyclic strain method. National Bureau of Standards, U.S. Department of Commerce, Wasington, D.C.
37. Figueroa JL, Dahisaria N (1991) An Energy approach in defining soil liquefaction. In: Proc Second Int Conf Recent Advances in Geotech Earthq Eng Soil Dyn Missouri, pp 407–410
38. Kokusho T (1980) Cyclic triaxial test of dynamic soil properties for wide strain range. Soils Found 20(2):45–60. https://doi.org/10.3208/sandf1972.20.2_45
39. Voznesensky EA, Nordal S (1999) Dynamic instability of clays: an energy approach. Soil Dyn Earthq Eng 18:125–133. https://doi.org/10.1016/S0267-7261(98)00043-8
40. Figueroa JL, Saada AS, Liang L, Dahisaria NM (1994) Evaluation of soil liquefaction by energy principles. ASCE J Geotech Eng 120(9):1554–1569. https://doi.org/10.1061/(ASCE)0733-9410(1994)120:9(1554)
41. Law KT, Cao YL, He GN (1990) An energy approach for assessing seismic liquefaction potential. Can Geotech J 27:320–329. https://doi.org/10.1139/t90-043
42. Nemat SN, Shokooh AA (1979) Unified approach to densification and liquefaction of cohesionless sand in cyclic shearing. Can Geotech J 16:659–678. https://doi.org/10.1139/t79-076
43. IS 1893 (part 1) (2016) Criteria for earthquake resistant design of structures. New Delhi.
44. Pandian NS, Rajasekhar C, Sridharan A (1998) Studies of the specific gravity of some Indian coal ashes. ASTM J Test Eval 26(3):177–186. https://doi.org/10.1520/JTE11990J

45. IRC 36 (2010) Recommended practice for earth embankments and subgrade for road works. New Delhi.
46. ASTM D5311-13 (2013) Standard test method for load controlled cyclic strength of soil. West Conshohocken, PA
47. ASTM D3999-11e1 (2013) Standard methods for the determination of the modulus and damping properties of soils using the cyclic triaxial apparatus. West Conshohocken, PA
48. Chattaraj R, Sengupta A (2016) Dynamic properties of fly ash. J Mater Civ Eng 29(1):04016190. https://doi.org/10.1061/(ASCE)MT.1943-5533.0001712
49. Saxena SS, Reddy KR (1989) Dynamic modulii and damping ratios for Monterey No. 0 sand by resonant column tests. Soils Found 29(2):37–51. https://doi.org/10.3208/sandf1972.29.2_37
50. Kumar SS, Krishna AM, Dey A (2017) Evaluation of dynamic properties of sandy soil at high cyclic strains. Soil Dyn Earthq Eng 99:157–167. https://doi.org/10.1016/j.soildyn.2017.05.016
51. Salgado R, Bandini P, Karim A (2000) Shear strength and stiffness of silty sand. J Geotech Geoenviron Eng 126:451–462
52. Thevanayagam S, Shenthan T, Mohan S, Liang J (2002) Undrained fragility of clean sands, silty sands and sandy silts. J Geotech Geoenviron Eng 128(10):849–859. https://doi.org/10.1061/(ASCE)1090-0241(2002)128:10(849)
53. Govindaraju L (2005) Liquefaction and dynamic properties of sandy soils. (Ph.D. thesis) Indian Institute of Science Bangalore.
54. Matasovic N, Vucetic M (1993) Cyclic characterization of liquefiable sands. J Geotech Geoenviron Eng 119(11):1805–1822. https://doi.org/10.1061/(ASCE)0733-9410(1993)119:11(1805)
55. Kiku H, Yoshida N (2000) Dynamic deformation property tests at large strains. In: Proc 12th World Conf Earthq Eng Newzealand, pp 1–7
56. Brennan AJ, Thusyanathan NI, Madabhushi SPG (2005) Evaluation of shear modulus and damping in dynamic centrifuge tests. J Geotech Geoenviron Eng 131:1488–1497. https://doi.org/10.1061/(ASCE)1090-0241(2005)131:12(1488)
57. Mashiri MS (2014) Monotonic and cyclic behavior of sand-tyre chip (STCh) mixtures (Ph. D. thesis). School of Civil, Mining and Environmental Engineering University of Wallongong, Australia